ChemComm

Chemical Communications

ROYAL SOCIETY
OF **CHEMISTRY**

COMMUNICATION
Julia L. Brumaghim *et al*.
Developing non-radioactive, radical methods to screen for
radiolytic stability

60 YEARS
ANNIVERSARY

ChemComm

Check for updates

Developing non-radioactive, radical methods to screen for radiolytic stability†

Brandon G. Wackerle, ‡[a] Madison R. Vicente, ‡[a] Fatema Tuz Zohara, [a]
Dean R. Peterman, [b] Modi Wetzler [a] and Julia L. Brumaghim *[a]

Radiolytically generated radicals cause degradation of nutrients in food, materials in satellites and solar cells, and human health. Radiation effects are studied using gamma radiolysis, a low-throughput, high-cost, and low-accessibility method. We developed a higher-throughput, low-cost, non-radioactive, radical assay that produces radicals similar to those generated in gamma radiolysis and examined monoamide degradation. Our radical assay results correspond to those from gamma irradiation in both monoamide stability and decomposition products, establishing this radical assay as a proof-of-concept screening tool for radiolytic stability.

Quantifying and predicting radiation effects on materials and biological samples has been a major undertaking for decades. The gold standard for studying gamma radiation effects and applications is irradiators with radioactive ^{60}Co or ^{137}Cs sources. These irradiators are used to initiate polymerization[1,2] and nanoparticle synthesis,[3] to sterilize food and medical products,[4] to develop materials for advanced solar cell technology and space travel,[5] and for tumor ablation with Gamma Knife®.[6] However, such irradiators are expensive, low-throughput, and under increasingly tight control due to radiological terrorism concerns.[7] Therefore, a safer and higher throughput method to semi-quantitatively predict gamma irradiation impacts is increasingly needed across a wide range of applications.

Since radicals produced in gamma radiolysis are the primary damaging species, chemically generating these radicals in an assay could provide a screening tool for radiolytic stability. We used our expertise in predicting and quantifying radical-mediated damage[8,9] to develop such a non-radioactive, radical assay. Initial testing of this assay requires a system where radiation and radical chemistry are well known, and no system

is more studied for radiation damage than nuclear extractants.[10] Monoamide extractants are proposed to replace tributyl phosphate (TBP; Fig. 1) to recover uranium and plutonium for reuse as nuclear fuel.[10] This interest has led to a large body of recent literature examining monoamide radiolytic stability and degradation products,[11–13] so they provide an excellent test case for developing the first non-radioactive, radical assay to predict radiolytic damage.

The most widely studied monoamide extractants are *N,N*-di(2-ethylhexyl)butyramide (DEHBA) and its isomer *N,N*-di(2-ethylhexyl)isobutyramide (DEHiBA; Fig. 1). α-Carbon branching variations alter their selectivity (DEHBA co-extracts U and Pu, whereas DEHiBA extracts U)[14] and radiolytic stability. Gamma radiolytic degradation of these monoamides in *n*-dodecane is very well studied, showing up to 20–30% decomposition at absorbed doses > 600–1000 kGy,[11,12] in comparison to similar degradation at ~ 100 kGy or less for many other classes of extractants.[15] At the other extreme, vitamins C and B2 (riboflavin) degrade at doses as low as 0.5–50 kGy.[16,17] While monoamide stability is advantageous for nuclear waste separations, irradiation of these monoamides to examine degradation can take up to one month in aging gamma irradiators, highlighting the need for rapid and less expensive screening methods.

In radiolysis, degradation is caused by radical species such as hydroxyl radical (•OH) and superoxide ($O_2^{•-}$) generated in aqueous, oxygenated solution and radical cations ($R^{•+}$) generated in organic solution.[18] To form similar radical species chemically, which would provide correspondence to radiolysis, we used an organic-soluble 2-(*tert*-butylazo)-2-hydroperoxypropane (azoperoxide)[19]
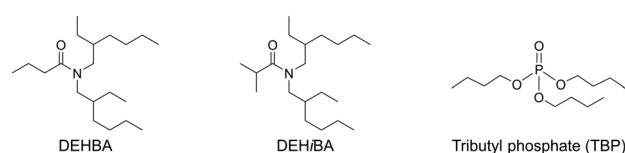
[a] Department of Chemistry, Clemson University, Clemson, SC 29634-0973, USA.
  E-mail: brumagh@clemson.edu
[b] Aqueous Separations and Radiochemistry Department, Idaho National Laboratory
  Idaho Falls, ID, 83415-6158, USA

† Electronic supplementary information (ESI) available. See DOI: https://doi.org/10.1039/d4cc03762f

‡ These authors contributed equally to this work.

Fig. 1 *N,N*-Di-(2-ethylhexyl)butyramide (DEHBA), *N,N*-di-(2-ethylhexyl)-isobutyramide (DEHiBA), and tributyl phosphate (TBP).
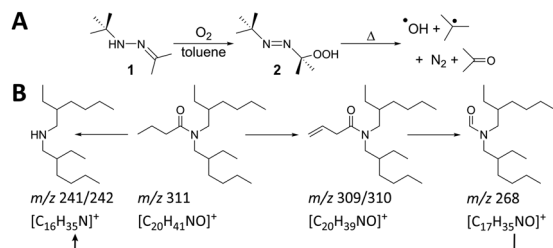
Scheme 1 (A) Formation of $^\bullet$OH and t-butyl radicals by thermal decomposition of azoperoxide **2** and (B) proposed DEHBA degradation pathways.

(**2**) to generate hydroxyl and alkyl radicals (Scheme 1A). Monoamide degradation using this method was examined by adding **2** (0–400 mM) to DEHBA or DEHiBA solutions (100 mM) in toluene, heating for 2 h at 75 °C, and observing the degradation products using gas chromatography-mass spectrometry (GC-MS).

Monoamide degradation products were identified by comparing total-ion chromatograms (TICs; Fig. 2 and Table S1, ESI†) of azoperoxide-treated monoamide samples and azoperoxide-treated toluene controls. Some products with the same m/z parent ion eluted at different, but close (typically within 1–2 min) retention times (Table S1, ESI†), suggesting isomer formation. Isomer formation is supported by density functional theory (DFT) calculations, showing that monoamide radical formation energies are within a similar 32–45 kJ mol^{-1} at different sites (Tables S3 and S4, ESI†). Integrating the TIC peaks provided relative percentages for the monoamide degradation products, and isomer peaks with identical m/z values were integrated together in the data analysis. For each identified degradation product, we have illustrated a possible structure based on the empirical formula and observed m/z (selected mass spectra are shown in Fig. S13, ESI†), but isomers of these products are also possible. For DEHBA, 18 to 44 degradation products with normalized TIC peak area percentages $\geq 1\%$
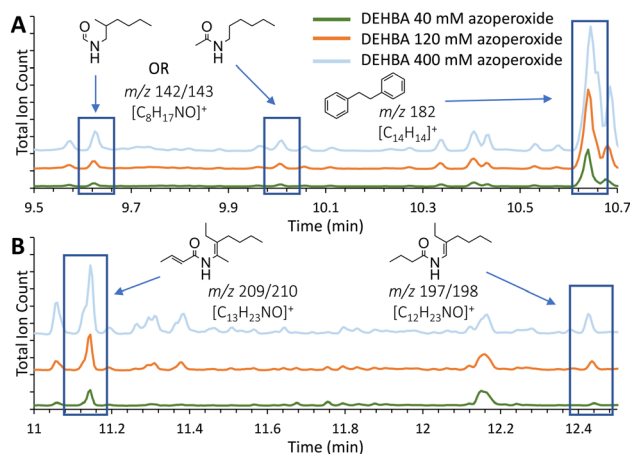

Fig. 2 (A) and (B) Insets of total-ion chromatograms (TICs) of DEHBA treated with azoperoxide in toluene, showing degradation products identified by GC-MS. Full TICs of DEHBA treated with all azoperoxide concentrations are provided in Fig. S7 (ESI†), with degradation products listed in Table S1 (ESI†). Equivalent DEHiBA data are depicted in Fig. S8 and S9 (ESI†). Trials were performed in triplicate with TIC relative standard deviations ranging from 2.5 ± 2.7% to 4.9 ± 3.3% (Table S2, ESI†).

were identified, with a greater number of degradation products observed with increasing azoperoxide concentration (40, 120, and 400 mM; Table S1, ESI†). TICs for azoperoxide-treated DEHBA generally show dose-dependent degradation product formation (Fig. 2).

DEHBA degrades into several major products, including those with m/z 197/198 ($[C_{12}H_{23}NO]^+$), 209/210 ($[C_{13}H_{23}NO]^+$), and 298 ($[C_{19}H_{39}NO]^+$, Fig. 2 and 3). Most DEHBA degradation products increase with increasing azoperoxide dose (40–400 mM), such as amide-H$_2$ (m/z 309/310 $[C_{20}H_{39}NO]^+$; Scheme 1B). In contrast, a few degradation products decrease with increasing dose, such as one with m/z 282 ($[C_{19}H_{25}NO]^+$), indicating further degradation into other products (Fig. 3A).

Radical degradation of DEHBA and DEHiBA show generally similar trends and products. Differences are observed, such as greater formation of the aldehyde with m/z 268 ($[C_{17}H_{35}NO]^+$; Scheme 1B) for DEHiBA than DEHBA, likely due to formation of a more substituted carbon radical upon dissociation of the α-branched C4 substituent (Fig. S14 and S15, ESI†). Similarly, the degradation product with m/z 142/143 ($[C_8H_{17}NO]^+$, Fig. 2) is also formed more for DEHiBA than DEHBA.

In contrast, the degradation product corresponding to amide-H$_2$ (m/z 309/310) forms more from DEHBA than DEHiBA, likely indicating a more stable dehydrogenated product. Additionally, monoamide-tolyl adducts (*e.g.*, m/z 282 and 401, $[C_{27}H_{47}NO]^+$) and bibenzyl (m/z 182, $[C_{14}H_{14}]^+$ formed from two tolyl radicals) are also observed. Two products remain unidentified (m/z 133 and 229; Table S1, ESI†).

To determine if monoamide degradation products formed during the non-radioactive, radical assay are similar to those formed during gamma radiolysis, we irradiated DEHBA and DEHiBA (100 mM, 0 to ~1000 kGy) in toluene using a ^{60}Co irradiator and analyzed the products by the same GC-MS methods. More degradation products form during irradiation than radical treatment, with 38 to 111 different degradation products of peak area $\geq 1\%$ identified (Fig. S16 and S17, ESI†). Increasing gamma irradiation dose generally leads to an increase in degradation products (Fig. 3B and 4), such as amine (m/z 241/242, $[C_{16}H_{35}N]^+$) and amide-H$_2$ (m/z 309/310). Degradation products with m/z 254/255 ($[C_{16}H_{33}NO]^+$), 268, and 282 show decreasing TIC peak area percentages between 42 and 1043 kGy irradiation (Fig. 3B), indicating further degradation of the initial degradation products formed.

Similar gamma radiolytic degradation products are seen for DEHBA and DEHiBA (Fig. S16 and S17, ESI†), with the amine (m/z 241/242) being the largest. DEHBA and DEHiBA also degrade into products with m/z 142/143, 169/170 ($[C_{10}H_{19}NO]^+$), 268, and 309/310 (Table S1, ESI†), often with varying percentages. For example, formation of m/z 268 and 309/310 degradation products (Scheme 1B) is greater for DEHBA than DEHiBA at ~1000 kGy, but formation of the m/z 169/170 degradation product is greater for DEHiBA than DEHBA (Table S1, ESI†). Two products (m/z 181, $[C_{11}H_{19}NO]^+$ and 188, $[C_{12}H_{13}NO]^+$) only form from DEHiBA degradation (Table S1). Solvent adducts also form during radiolytic degradation, such as the amide–tolyl adduct (m/z 401). As in the

Fig. 3 Graphs showing major DEHBA degradation products upon treatment with (A) azoperoxide and (B) gamma radiation. Major products have ≥6% normalized area percentages for at least one of the three doses. (C) Comparison of DEHBA degradation products from 120 mM azoperoxide or 412 kGy gamma radiation treatment (≥1% normalized area percentages for either treatment). Equivalent comparison for DEHiBA is depicted in Fig. S18 (ESI†). Degradation products and percentages are listed in Table S1 (ESI†). Trials were performed in triplicate with TIC relative standard deviations ranging from 2.5 ± 2.7% to 4.9 ± 3.3% for the radical assay and 3.4 ± 3.0% to 5.0 ± 7.0% for gamma radiolysis.
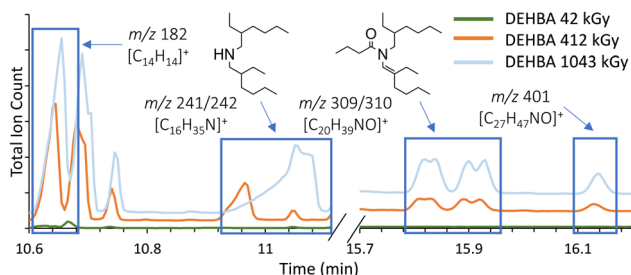
Fig. 4 Inset of total-ion chromatograms (TICs) of gamma irradiated DEHBA in toluene showing degradation products identified by GC-MS (intensity left of the break is 6×10^7 and 3×10^7 on the right). Full TICs for DEHBA at all radiation doses are provided in Fig. S10 (ESI†), with degradation products listed in Table S1 (ESI†). Equivalent DEHiBA data are depicted in Fig. S11 and S12 (ESI†). Trials were performed in triplicate with TIC relative standard deviations ranging from 3.4 ± 3.0% to 5.0 ± 7.0%.

radical assay, bibenzyl is also a major toluene degradation product.

DEHBA and DEHiBA form similar degradation products in the gamma radiolysis and radical assays through similar pathways (Table 1 and Scheme 1B) despite their differences in radical generation. In both methods, monoamides degrade to products with m/z of 114 ($[C_6H_{11}NO]^+$), 197/198, 212 ($[C_{13}H_{25}NO]^+$), 241/242, 252 ($[C_{17}H_{33}N]^+$), 268, 282, 306 ($[C_{20}H_{35}NO]^+$), 309/310, and 401 (Fig. 3C). In most cases, more degradation products at higher concentrations are formed by gamma radiolysis, due to higher achievable doses in gamma radiolysis than in the radical assay, but degradation products with m/z 197/198 and 282 form in greater relative percentages in the radical assay (Fig. 3C).

To quantify DEHBA degradation as is typical for irradiation studies,[12] the DEHBA FID peak was integrated to determine amide concentration as a function of gamma radiation dose (Fig. S19–S22, ESI†). A dose constant of $2.4 \pm 0.8 \times 10^{-4}$ kGy^{-1} was calculated for DEHBA (Fig. S23, ESI†), consistent with a value of $2.7 \pm 0.3 \times 10^{-4}$ kGy^{-1} reported for irradiation in dodecane.[20] Degradation dose constants were not obtained from DEHiBA irradiation (Fig. S24, ESI†) or DEHBA and DEHiBA radical assay results since these monoamides do not show statistically sufficient degradation under these conditions. DFT calculations also indicate that DEHiBA is more stable than DEHBA (Tables S3 and S4, ESI†).

Table 1 Comparison of DEHBA and DEHiBA degradation products from gamma radiolysis and radical assay studies in toluene and from literature reports in dodecane.[11–13] Structures of degradation products are shown in Scheme 1 and Fig. 2, 3

Degradation product (m/z)	In gamma radiolysis?	In radical assay?	Reported in dodecane?
C–N bond cleavage–H₂ (197/198)	YES[a]	YES	YES[a]
N–CO & C–H bond cleavages (240)	YES	YES[a]	YES
N–CO bond cleavage (241/242)	YES	YES[b]	YES
Cleavage of C-terminus (268)	YES	YES	NO
Monoamide–H₂ (309/310)	YES	YES	YES
Monoamide + tolyl adduct (401)	YES	YES	YES[c]
Unidentified (133)	YES	YES[b]	NO

[a] DEHiBA only. [b] DEHBA only. [c] Dodecyl adduct.

Unsurprisingly, the two methods show some differences in monoamide degradation products (Fig. 3C and Fig. S18, ESI†) due to differences in radicals generated in each system and the greater degradation achievable during gamma radiolysis. For example, the DEHBA degradation product with m/z 268 is the largest in the radical assay at the highest dose (400 mM azoperoxide; Table S1, ESI†) and increases with increasing azoperoxide dose. The opposite trend is observed for radiolysis; the degradation product with m/z 268 is greatest at the lowest radiolysis dose (42 kGy, Table S1, ESI†) and decreases with increasing dose.

The generally similar products formed in our radical assay and radiolysis experiments in toluene also compare favorably to previously reported monoamide degradation products from radiolysis in aqueous, nitric-acid-contacted n-dodecane (Table 1).[11–13] Although hydroxyl radical is not formed in gamma radiolysis of toluene, tolyl radicals, the most concentrated radical in both methods, degrade monoamides similarly to form the degradation products (Scheme 1B).

Bibenzyl forms in both the radical and gamma radiolytic studies from toluene degradation, and its concentration was quantified by GC-MS (Fig. S25 and S26, ESI†). In all cases, bibenzyl formation is linear with dose (Fig. 5). In the irradiated samples, bibenzyl formation is lower for the toluene-only control than the monoamide-containing samples (Fig. 5A). This is unsurprising, since radiolytic stability can depend on sample
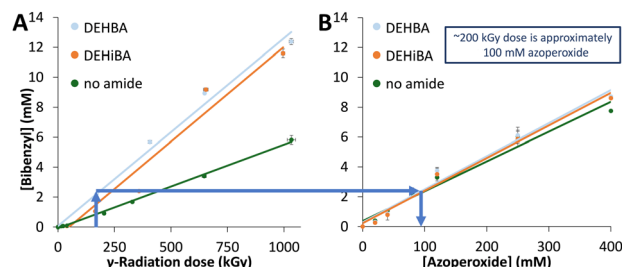
Fig. 5 (A) Absorbed gamma radiolysis dose compared to (B) radical assay azoperoxide concentration showing estimated correspondence using bibenzyl formation in toluene. Error bars represent results of trials performed in triplicate.

purity,[21,22] and in this system, the monoamide is an impurity in the toluene solvent. In the radical assay, the 'no monoamide' control includes radical-generating azoperoxide, and therefore shows similar bibenzyl formation compared to the monoamide-containing samples. Comparing bibenzyl concentrations as an internal standard allows us to compare radical and radiolytic methods, so that, for example, an azoperoxide concentration of 100 mM is estimated as an absorbed radiation dose of approximately 200 kGy (Fig. 5). This correlation also suggests that the highest azoperoxide dose in the radical assay (400 mM; limited by experimental methods) leads to $\sim$8 mM bibenzyl formation, similar to a $\sim$650 kGy irradiation. Thus, the maximum radiolytic dose (1000 kGy) produces more damage than the radical assay can achieve and forms more degradation products. This difference reinforces why there is no exact correlation in Fig. 3C, since $\sim$2.8 mM bibenzyl is formed upon 120 mM azoperoxide treatment, whereas $\sim$5.2 mM bibenzyl is formed after 412 kGy irradiation. This work represents the first correspondence between a non-radioactive radical assay and gamma radiolysis, providing relative radiolytic stabilities and estimated irradiation doses (0–650 kGy) for radiolytic studies.

In addition to similar trends in monoamide stability and degradation products in our radical assay compared to gamma radiolysis, this work represents a more comprehensive analysis of DEHBA and DEHiBA degradation than has previously been accomplished.[11–13] Up to 44 azoperoxide and 111 radiolytic degradation products are identified, more than twice as many as in previous reports.[11–13] This includes the determination of dose-dependence for each degradation product (Table S1, ESI†), and identification of previously unidentified products, such as the aldehyde with m/z 268 (Scheme 1B). The ability to conduct such a comprehensive analysis is critical in demonstrating the proof-of-concept utility of our higher throughput radical screening method for applications beyond nuclear waste separations, such as the formation of potentially toxic volatile organic compounds due to radiolytic degradation of organic and biological material in closed atmospheres of spacecraft and extraterrestrial habitats.[23] The ability of this radical assay to screen for radiolytic stability and estimate dose ranges for traditional radiolytic studies using only GC-MS methods has the potential to accelerate progress and broaden participation in fields as diverse as nuclear separations, food and medical

sterilization, polymer and nanoparticle stability, and spacecraft design.

Data availability

The data supporting this article are included as part of the ESI.†

Conflicts of interest

There are no conflicts to declare.

Notes and references

1 M. Jamalzadeh and M. J. Sobkowicz, *Polym. Degrad. Stab.*, 2022, **206**, 110191.
2 A. Ashfaq, M.-C. Clochard, X. Coqueret, C. Dispenza, M. S. Driscoll, P. Ulański and M. Al-Sheikhly, *Polymers*, 2020, **12**, 2877.
3 S. Ahmad, R. Hammad and S. Rubab, *J. Electron. Mater.*, 2022, **51**, 5550–5567.
4 B. Bisht, P. Bhatnagar, P. Gururani, V. Kumar, M. S. Tomar, R. Sinhmar, N. Rathi and S. Kumar, *Trends Food Sci. Technol.*, 2021, **114**, 372–385.
5 V. Romano, A. Agresti, R. Verduci and G. D'Angelo, *ACS Energy Lett.*, 2022, **7**, 2490–2514.
6 P. Palmisciano, C. Ogasawara, M. Ogasawara, G. Ferini, G. Scalia, A. S. Haider, O. Bin Alamer, M. Salvati and G. E. Umana, *Pituitary*, 2022, **25**, 404–419.
7 J. Kamen, W.-Y. Hsu, B. Boswell and C. Hill, *Health Phys.*, 2019, **117**, 558–570.
8 N. R. Perron and J. L. Brumaghim, *Cell Biochem. Biophys.*, 2009, **53**, 75–100.
9 M. T. Zimmerman, C. A. Bayse, R. R. Ramoutar and J. L. Brumaghim, *J. Inorg. Biochem.*, 2015, **145**, 30–40.
10 K. McCann, J. A. Drader and J. C. Braley, *Sep. Purif. Rev.*, 2018, **47**, 49–65.
11 J. Drader, G. Saint-Louis, J. M. Muller, M. C. Charbonnel, P. Guilbaud, L. Berthon, K. M. Roscioli-Johnson, C. A. Zarzana, C. Rae, G. S. Groenewold, B. J. Mincher, S. P. Mezyk, K. McCann, S. G. Boyes and J. Braley, *Solvent Extr. Ion Exch.*, 2017, **35**, 480–495.
12 G. P. Horne, C. A. Zarzana, T. S. Grimes, C. Rae, J. Ceder, S. P. Mezyk, B. J. Mincher, M.-C. Charbonnel, P. Guilbaud, G. Saint-Louis and L. Berthon, *Dalton Trans.*, 2019, **48**, 14450–14460.
13 J. A. Drader, N. Boubals, B. Camès, D. Guillaumont, P. Guilbaud, G. Saint-Louis and L. Berthon, *Dalton Trans.*, 2018, **47**, 251–263.
14 D. Prabhu, G. Mahajan and G. Nair, *J. Radioanal. Nucl. Chem.*, 1997, **224**, 113–117.
15 B. J. Mincher, G. Modolo and S. P. Mezyk, *Solvent Extr. Ion Exch.*, 2009, **27**, 579–606.
16 H. F. Ramírez-Cahero and M. A. Valdivia-López, *Food Chem.*, 2018, **245**, 1131–1140.
17 G. P. Jacobs, *Radiat. Phys. Chem.*, 2022, **190**, 109795.
18 J. W. T. Spinks and R. J. Woods, *An introduction to radiation chemistry*, John Wiley and Sons Inc., New York, NY, USA, 3 edn, 1990, pp. 243–451.
19 L. C. Moores, D. Kaur, M. D. Smith and J. S. Poole, *J. Org. Chem.*, 2019, **84**, 3260–3269.
20 B. J. Mincher and C. A. Zarzana, *Radiation Chemistry of Diethylhexylbutyramide (DEHBA)*, Office of Scientific and Technical Information (OSTI), 2017, pp. 1–11.
21 J. Chen, R. Jiao and Y. Zhu, *Solvent Extr. Ion Exch.*, 1996, **14**, 555–565.
22 I. Y. Fleitlikh, N. A. Grigorieva and O. A. Logutenko, *Solvent Extr. Ion Exch.*, 2018, **36**, 1–21.
23 O. Monje, S. Valling, J. Cornish and K. Rojdev, *43rd International Conference on Environmental Systems*, Vail, CO, USA, 2013.